HHS Public Access

Author manuscript

Acad Radiol. Author manuscript; available in PMC 2017 November 01.

Published in final edited form as:

Acad Radiol. 2016 November ; 23(11): 1349–1358. doi:10.1016/j.acra.2016.06.002.

Texture-based quantification of centrilobular emphysema and centrilobular nodularity in longitudinal CT scans of current and former smokers

Shoshana B. Ginsburg, **Jason Zhao**, **Stephen Humphries**, **Sungshick Jou**, **Kunihiro Yagihashi**, **David A. Lynch**, **Joyce D. Schroeder**, and **for the COPDGene Investigators**

Abstract

Rationale and Objectives—The effect of smoking cessation on centrilobular emphysema (CLE) and centrilobular nodularity (CN), two manifestations of smoking-related lung injury on CT images, has not been clarified. The objective of this study is to leverage texture analysis to investigate differences in extent of CLE and CN between current and former smokers.

Materials and Methods—Chest CT scans from 350 current smokers, 401 former smokers, and 25 control subjects were obtained from the multicenter COPDGene Study, a HIPAA-compliant study approved by the institutional review board of each participating clinical study center. Additionally, for 215 of these subjects, a follow-up CT scan was obtained approximately five years later. For each CT scan, 5000 circular regions-of-interest (ROIs) of 35-pixel diameter were randomly selected throughout the lungs. The patterns present in each ROI were summarized by fifty computer-extracted texture features. A logistic regression classifier was leveraged to classify each ROI as normal lung, CLE, or CN, and differences in the percentages of normal lung, CLE, and CN by study group were assessed.

Results—Former smokers had significantly more CLE ($p < 0.01$) but less CN ($p < 0.001$) than current smokers, even after adjustment for important covariates such as patient age, GOLD stage, smoking history, FEV_1, gas trapping, and scanner model. Among patients with longitudinal CT scans, continued smoking led to a slight increase in CLE ($p = 0.13$), whereas sustained abstinence from smoking led to further reduction in CN ($p < 0.05$).

Conclusion—The proposed texture-based approach quantifies the extent of CN and CLE with high precision. Differences in smoking-related lung disease between longitudinal scans of current and former smokers suggest that CN may be reversible upon smoking cessation.

Corresponding Author: Shoshana Ginsburg, Center for Computational Imaging and Personalized Diagnostics, Department of Biomedical Engineering, Case Western Reserve University, Ohio, USA, Address: 2071 Martin Luther King Drive, Cleveland, OH 44106, Phone: 216-368-8519, Fax: 216-368-4969, shoshana.ginsburg@case.edu.

Introduction

Chronic obstructive pulmonary disease (COPD) is the third leading cause of mortality in the United States (1) and is projected to be the fourth leading cause of mortality worldwide by 2030 (2). COPD, which is strongly associated with smoking, is characterized by persistent airflow obstruction and a reduced ratio of forced expiratory volume in 1 second to forced vital capacity (FEV_1/FVC). Currently the most effective treatment for COPD is smoking cessation, which slows down the progressive decline in lung function (3,4) and leads to a transient improvement in FEV_1 (5).

Smoking-related lung injury manifests on CT images as centrilobular nodularity (CN) and centrilobular emphysema (CLE). CN, or micronodules centered in the pulmonary lobule (6), is generally thought to represent smoking-related respiratory bronchiolitis and is the earliest and most common manifestation of smoking-related lung inflammation (7-13), which may subsequently lead to emphysema. CLE is associated with low attenuation values similar to the density of air due to the destruction of alveolar walls in lung tissue. The severity and extent of CLE and CN in patients with COPD is commonly assessed by radiologists reading CT images. Nevertheless, qualitative assessment of CT images for extent of CLE and, more notably, CN is associated with high inter-observer variability (14,15). For example, when 9-11 pulmonogists and radiologists reviewed each of 395 CT scans at the COPDGene Study CT Imaging Workshop in 2010, average κ values for quantifying CLE and CN were 0.33 and 0.12, respectively (15).

Whereas radiologist assessment of CT images is subject to high inter-observer variability (18,19), quantitative analysis of CT images facilitates precise and reproducible measurements. Densitometry is commonly used to quantify emphysema on CT images (16-19). However, densitometry may fail to detect mild degrees of CLE (15) and is not useful for detecting CN because smokers with CN may have overall normal lung density measurements. In contrast, texture-based methods have been introduced for quantifying both emphysema (20-22) and, more recently, CN (23). Using a texture-based approach, Ginsburg et al. (23) were able to classify CN and CLE regions-of-interest in the lung with 74% and 95% accuracy, respectively. With the advent of this approach it has for the first time become possible to quantify CN and thereby investigate the effects of treatment or smoking cessation on CN measurements in patients with COPD.

The effect of smoking cessation on CLE and CN has been studied only minimally, with conflicting results (5,12,24-26). While one study found that CLE decreased (24) and another found no significant change in CLE (5), quantitative studies found that the apparent amount of emphysema actually increased upon smoking cessation (probably due to a decrease in smoking-related inflammation resulting in lower lung attenuation) (25,26). Whereas CLE can be quantified via densitometry, the high inter-observer variability in radiologist assessment of CN has been a severe impediment to evaluating the effect of smoking cessation on CN. Only one study evaluated the effect of smoking cessation on CN (5); they found a reduction in the number of micronodules evident on CT after smoking cessation. However, in this study the percentage of lung affected by CN was estimated qualitatively by

radiologists. Thus, there is a need for quantitative analysis of the impact of smoking cessation on CN.

The purpose of this study was to investigate the differences in CN and CLE between current and former smokers and to evaluate the effect of smoking cessation on the extent of CN and CLE. On an independent training set, we trained a classifier to use 50 texture features to discriminate between textural patterns associated with CN, CLE, and normal lung tissue. After evaluating the precision of our texture-based classifier in quantifying the percentage of the lung affected by CN and CLE, we implemented this method to quantify CN and CLE in 776 patients from the COPDGene Study, including 401 former smokers, 350 current smokers, and 25 control subjects who never smoked. Additionally, for 139 former and 76 current smokers for which longitudinal CT scans were available we investigated changes in CN and CLE due to sustained smoking exposure and smoking cessation.

Materials and Methods

Subjects

Chest CT scans were obtained from the multicenter COPDGene Study (19), a cross-sectional study approved by the institutional review board of each of the 21 participating clinical study centers. All image management is compliant with the Health Insurance Portability and Accountability Act. The COPDGene Study recruited 10,300 subjects, including 10,192 current or former smokers and 108 non-smokers. All subjects in this study were non-Hispanic whites or African Americans aged 45-80 years with no history of concomitant respiratory disorders other than asthma or COPD and no known or suspected lung cancer. Additional details regarding inclusion and exclusion criteria can be found in the COPDGene study design paper (19).

From the COPDGene Study cohort, we randomly selected 500 subjects with mild to moderate COPD (GOLD stages -1/0/1/2), including 250 current smokers and 250 former smokers, as well as 25 control subjects who never smoked (27). Additionally, we included 100 current smokers and 151 former smokers who had undergone detailed visual CT scoring for severity of CLE and CN (28). An independent, randomly-selected training set including 22 current smokers, 18 former smokers, and 19 non-smokers was used for developing the textural algorithm and training the classifier. In order to minimize issues caused by inter-scanner differences, only subjects scanned on Siemens scanners (Definition, Definition-Flash, Definition-AS+, Sensation-64) (Siemens Inc, Forchheim, Germany) were considered for this study. Thus, in total, 776 subjects were included: 350 current smokers, 401 former smokers, and 25 control subjects. Of these 776 subjects, 215 (139 former and 76 current smokers) returned approximately five years later for follow-up CT scans in Phase 2 of the COPDGene Study. Table 1 provides a more detailed description of the subjects included in this study.

Image Acquisition

All subjects underwent volumetric chest CT imaging at full inspiration. CT scans were reconstructed with a slice thickness of 0.75 mm and a slice interval of 0.5 mm to achieve

near isotropic voxels. Scans were acquired at 200 mAs and 120 kVp. A B31f reconstruction kernel was used to achieve medium smooth images. All scans underwent quality assurance by a trained research analyst to ensure compliance with study protocol, adequacy of inspiration, inclusion of all parts of the chest, and absence of motion artifact (19,29).

Radiologist Assessment

For 100 former and 151 current smokers, visual scoring of Phase 1 CT scans was performed independently by two radiologists with 7 and 12 years of experience reading chest CT images. The extent of CLE and CN was assessed according to a five-point scale in each of the five lobes and lingula: absent, <25%, 25% to 50%, 50% to 75%, and > 75% When the two radiologists' scores did not agree, the mean of the two readings was used for this study. The mean scores were then summed for all lobes and the lingula, so that the final radiologist score was on a 30-point scale.

Classifier Training

A classifier was trained to distinguish between patterns of normal lung, CLE, and CN based on a set of regions-of-interest (ROIs) selected by a chest radiologist with 6 years of experience. From the 59 subjects in the training cohort (see Table 1), a total of 868, 724, and 640 non-overlapping circular ROIs of 35-pixel diameter were selected that illustrated normal lung, CLE, and CN, respectively. These ROIs were reviewed by a second chest radiologist (11 years of experience), who confirmed that each ROI was correctly labeled as normal lung, CLE, or CN. In order to ensure that the ROIs illustrating normal lung patterns included a diverse set of normal lung patterns, an additional 50 ROIs were randomly selected throughout the lung parenchyma of each of the non-smoking training subjects and were used to augment the training set. The patterns present in each ROI were summarized by fifty computer-extracted features describing the underlying textures of the lung parenchyma. These features, listed in Supplementary Table 1, included 10 first-order statistics and 22 run length and gap length features previously shown to be useful for distinguishing between normal lung, CLE, and CN (23). In addition, 18 features, designed to model the shapes and intensity distributions of both regions of CLE (i.e., low attenuation areas) and micronodules associated with CN (i.e., high attenuation areas), were computed for each ROI. Further details regarding the computation of these 18 radiology-derived features can be found in Appendix 1. These fifty texture features were used to train a logistic regression classifier (30) to accurately classify the ROIs in the training set as normal lung, CLE, and CN. When implemented in a six-fold cross-validation framework, the trained classifier accurately classified 95.9%, 93.7%, and 86.3% of ROIs depicting normal lung, CLE, and CN, respectively (see Figure 1). All image analysis and classifier training steps were performed using Matlab R2013a (The Mathworks, Inc., Natick, MA).

Classifier Precision Analysis

Since the classifier would be applied to quantify the amount of normal lung, CLE, and CN present in a subject's CT scan, we sought to identify the number N of randomly selected ROIs that is necessary to ensure precision and reproducibility of the percentages of normal lung, CLE, and CN provided by the logistic regression classifier. Specifically, our objective was to determine the value of N for which the percentages of normal lung, CLE, and CN

would not vary between repetitions by more than one percentage point. Consequently, for each subject in the training cohort random selection and subsequent classification of *N* ROIs was repeated 10 times, and the variability in the percentage of ROIs classified as normal lung, CLE, and CN was assessed. ROIs were selected by randomly sampling an *x*, *y*, and *z* coordinate within the lung parenchyma; thus, the selected ROIs were uniformly distributed across the entire lung. Values of N=1000, 2500, and 5000 were considered. When 5000 ROIs were randomly selected for texture analysis and classification, standard deviations in percentages of normal lung, CLE, and CN remained below one percentage point for all 59 training subjects (see Figure 2). Consequently, for all subsequent analyses 5000 ROIs were randomly selected for each CT scan in order to cap variability at one percentage point.

Texture-Based CT Analysis

Automated segmentation of the right and left lungs from the chest wall and mediastinum was performed on all 776 CT scans in the evaluation cohort, as well as the 215 follow-up CT scans, using Pulmonary Workstation Plus (VIDA Diagnostics, Inc., Coralville, IA). All subsequent image analysis was performed using Matlab R2013a (The Mathworks, Inc., Natick, MA). For each CT scan 5000 circular ROIs of 35-pixel diameter were randomly selected throughout the lungs. Heuristics were implemented to ensure that the selected ROIs (a) did not contain large airways by limiting the number of voxels with HU>-850 and (b) were sufficiently far from the periphery by ensuring that at least 95% of each ROI was contained in the lung parenchyma. Fifty texture features, listed in Supplementary Table 1, were calculated for each ROI; in conjunction with the trained logistic regression classifier, these fifty features were used to classify each ROI as normal lung, CLE, or CN. Finally, percentages of normal lung, CLE, and CN were obtained for each subject.

Statistical Analysis

Differences in the percentages of normal lung, CLE, and CN by study group were assessed using the two-sample Student's *t*-test. The effect of confounding factors, such as disease severity (FEV_1), age, smoking duration, GOLD stage, gas trapping, and differences in scanner model, on differences between study groups was evaluated via multivariate regression analysis. Additionally, the two-sample Student's *t*-test was used to assess differences in the percentages of CN and CLE between longitudinal CT scans. Correlations between percentages and clinical features were calculated using Pearson's correlation coefficient. Because visual scores were ordinal, Spearman's rank correlation was used to assess correlations between percentages of normal lung, CLE, and CN and visual scores. All statistical analyses were performed using Matlab R2014b (The Mathworks, Inc., Natick, MA).

Results

One hundred randomly selected ROIs from a single subject in the test set, as well as the results of classifying these ROIs by the logistic regression classifier, are shown in Figure 3. The percentages of ROIs classified as normal lung, CLE and CN for nonsmokers, former smokers, and current smokers are shown in Figure 4. Both former and current smokers had significantly fewer normal ROIs than nonsmokers (see Table 2), although there is no

difference in the amount of normal ROIs in former versus current smokers. An average of 96.6% of ROIs from the CT scans of nonsmokers were classified as normal, compared to 78.6% and 80.6% in former and current smokers, respectively. In contrast, an average of 2.3% of ROIs in nonsmokers were classified as CN, compared to 4.5% in former smokers and 9.8% in current smokers. Also, an average of 1.2% of ROIs in nonsmokers were classified as CLE, 16.9% and 9.6% were classified as CLE in former and current smokers, respectively. Both former and current smokers had significantly more CLE ROIs than nonsmokers, and current smokers had significantly more CN ROIs than nonsmokers. Compared to current smokers, former smokers had significantly more CLE ROIs but fewer CN ROIs. These differences between current and former smokers remained statistically significant ($p < 0.01$) when confounding factors such as disease severity (FEV_1), age, smoking duration, GOLD stage, gas trapping, and differences in scanner model were accounted for. Percentages of CLE and CN were somewhat affected by scanner model; specifically, the Siemens Sensation-64 scanner provided significantly different percentages of CN and CLE than the other Siemens scanners ($p < 0.01$). However, differences in scanner model had an insignificant effect on measurements of CLE ($p = 0.52$) and CN ($p = 0.15$) when other factors—age, GOLD stage, pulmonary function, gas trapping, and smoking history—were considered.

The percentage of ROIs with CLE correlated strongly with both visual CLE scores ($\rho = 0.84$, see Figure 5) and the amount of emphysema according to densitometry ($\rho = 0.75$). In contrast, percentage of ROIs with CN correlated only moderately with visual CN scores ($\rho = 0.31$). The percentage of CLE ROIs increased with GOLD stage and was inversely related to both lung function and time since smoking cessation (see Table 4). The percentage of ROIs with CN was inversely related to GOLD stage, as well as the percentages of emphysema and gas trapping according to densitometry (see Table 4). Percentage of CN ROIs was unrelated to lung function and time since smoking cessation.

Of 139 former smokers who returned for a follow-up CT scan, 134 remained abstinent while 5 started smoking again prior to their follow-up CT scan. Former smokers who remained abstinent had significantly fewer CN ROIs in Phase 2 than Phase 1 (see Table 3 and Supp. Figure 1), although the number of CLE ROIs did not change significantly between CT scans. The high proportion of CN ROIs in current smokers persisted on longitudinal follow-up in those who continued to smoke. No significant difference in percentage of CN or CLE ROIs was found in those who quit smoking or in those who restarted smoking, perhaps due to small numbers in these groups (see Table 3 and Figure 6). Current smokers in Phase 1 who continued to smoke in Phase 2 saw further increase in percentage of CLE, although this difference was not statistically significant ($p = 0.13$).

Discussion

In this study we leveraged computer-extracted texture features and trained a logistic regression classifier to quantify the extent of CLE and CN present in CT scans. This classifier was applied to calculate the percentage of lung affected by CLE and CN in 776 former and current smokers in the COPDGene Study and, thereby, to investigate differences in CLE and CN between current and former smokers. Additionally, longitudinal changes in

percentages of lung affected by CLE and CN were evaluated on 215 smokers, many of whom remained abstinent from smoking and some of whom ceased smoking between longitudinal CT scans.

Although both former and current smokers had the same overall amount of ROIs showing CLE or CN ($p = 0.21$), the CT manifestations of COPD appeared to be different for these two groups (see Table 2). While former smokers had fewer CN ROIs than current smokers, they also had more than twice as many CLE ROIs as current smokers. These differences in the amount of CLE and CN ROIs were statistically significant ($p < 0.01$) even when controlling for the effects of age, GOLD stage, lung function, amount of gas trapping, smoking duration, and scanner model. These findings echo previous studies, which reported a reduction in the presence of CN on CT following smoking cessation (5) and an increase in the apparent amount of quantitative emphysema in former versus current smokers (24). The latter trend may be attributed in part to the "healthy smoker effect" (31), where current smokers are, in general, healthier than former smokers because subjects who experience respiratory symptoms quit smoking. In fact, in our study cohort former smokers had reduced lung function (measured by FEV_1) compared to current smokers ($p < 0.01$), corroborating the "healthy smoker effect". Additionally, due to the partial volume effect, smoking-induced inflammation can mask emphysema in current smokers.

Even apparently healthy smokers who do not experience abnormal lung function can manifest CLE (5) or CN (5,25) on CT images. In fact, we found that control subjects who never smoked had an average of 1.1% and 2.3% CLE and CN, respectively. It is interesting to note that the percentage of CN in former smokers was not significantly different from the percentage of CN in nonsmokers, which suggests that CN may be reversible upon smoking cessation. However, a prospective study would be necessary to prove this.

Former smokers in Phase 1 who remained abstinent from smoking in Phase 2 of the COPDGene Study saw significant further reduction in the number of CN ROIs on their Phase 2 scans. This further corroborates the idea that CN may actually be reversible. Nevertheless, no reduction in the percentage of lung affected by CN was seen in smokers who quit smoking between Phases 1 and 2, possibly due to the small number of such subjects.

The gold standard for measuring CLE and CN is radiologist assessment. Although percentage of CLE correlated strongly with both visual CLE scores and densitometric measures of emphysema, correlation with visual scores was stronger ($\rho = 0.84$ compared to $\rho = 0.75$). This supports the idea that texture features more closely model radiologists' visual processes than densitometry. The percentage of CN found by our approach was only moderately correlated with visual CN score. This may be due to the fact that CN is a subtle pattern that is not detected and quantified consistently by radiologists (15) or due to blood vessels being misclassified as CN.

In order to assess changes in percentages of CLE and CN due to disease progression, therapy, or smoking cessation, precise percentages are requisite. Our approach, which involved randomly selecting and classifying 5000 ROIs in each CT scan, resulted in highly

precise measurements of CN and CLE; standard deviations in repeated measurements of percentages of normal lung, CN, and CLE were consistently below one percentage point. This small amount of variation was due to the fact that a subset of ROIs was randomly selected to represent the entire lung parenchyma. Thus, repeated tests result in different sets of randomly selected ROIs and hence slightly different measurements of CN and CLE. In comparison, densitometry, which involves the analysis of every voxel in the lung, is more precise. However, simple density measurements are ineffective for detecting CN because smokers with CN may have overall normal lung intensities. Consequently, our approach is the first that is capable of precisely quantifying both CN and CLE, two distinct manifestations of COPD on CT images.

Nevertheless, there were several limitations to our study. Firstly, the performance of the classifier is limited by the quality of training patterns selected and labeled by radiologists. Although the radiologists who trained our classifier had 6 and 11 years of experience in thoracic radiology, radiologist detection of CN and CLE is known to be subjective and inconsistent (15). This may have negatively affected classifier performance. Secondly, subjects included in our study were not age-matched, and former smokers were, on average, seven years older than current smokers. Nevertheless, the effect of age-related differences between former and current smokers was accounted for in our statistical analysis. Thirdly, four different scanner models were used for image acquisition in this study, although it is well-known that densitometric measures of CLE are dependent on scanner model and reconstruction kernel (23,32,33). In fact, we found that differences in scanner model may have impacted texture-based measurements of CN and CLE, although this effect was masked by confounding factors. In particular, CLE and CN measures obtained from images acquired on a Siemens Sensation 64 scanner were significantly different from CLE and CN measures obtained on the other three Siemens scanners. Nevertheless, this effect of differences in scanner model on texture measures could probably be mitigated by applying intensity standardization to the HU intensities prior to texture analysis. Also, since the current study included only subjects scanned with Siemens scanners with 64 or more detector rows, further training and development will be necessary to apply this technique to other scanner makes and to scans obtained at lower radiation doses. Fourthly, since this study assessed texture patterns on 2-dimensional images, it is fundamentally limited in its ability to differentiate CN from small vascular structures. This limitation could be overcome by analyzing texture patterns in 3 dimensions. In conclusion, the proposed texture-based approach was shown to quantify the extent of CN and CLE with high precision, providing the potential to enable tracking of disease progression and response to therapy. This study found that CT manifestations of COPD are significantly different between current and former smokers. Our findings that former smokers have less CN than current smokers and that sustained abstinence leads to further reduction in the amount of CN suggests that CN may be reversible upon smoking cessation.

Supplementary Material

Refer to Web version on PubMed Central for supplementary material.

Acknowledgments

Funding agencies: This work was made possible by grants from the National Institutes of Health under award numbers R01 HL089856 and R01 HL089897.

Appendix

The central tenet underlying the computation of radiology-derived features is that although CN is associated with high attenuation values and CLE is associated with low attenuation values, not all high attenuation values indicate CN and not all low attenuation values indicate CLE. Rather, the sizes and characteristics of regions of high and low intensities are crucial for accurate detection of CN and CLE, respectively. A threshold of -950 HU has been shown to be the most valid threshold for defining emphysema (34). Consequently, we define a low attenuation area (LAA) as a region with at least sixteen connected voxels with HU <-950. Since the milder forms of emphysema are associated with intensities below -856 HU (35), a high attenuation area (HAA) is defined as a region with at least five connected voxels with HU >-850 in order to capture small centrilobular nodules.. Once LAAs and HAAs have been automatically identified within an ROI, seven LAA-based features and seven HAA-based features are extracted from each ROI:

- Number of LAAs/HAAs
- Mean size of LAAs/HAAs
- Mean intensity within LAAs/HAAs
- Mean background intensity outside of LAAs/HAAs
- Contrast between background intensity and intensity within LAAs/HAAs
- Mean of minimum intensity within LAAs/HAAs
- Intensity range within LAAs/HAAs

Additionally, the area immediately surrounding HAAs was found to aid in CN detection. In order to emphasize centrilobular nodules, high attenuation gradient areas (HAGAs) were identified as HAAs combined with surrounding voxels with gradient values >350 HU. Four HAGA-based features were then calculated:

- Mean intensity with HAGAs
- Mean background intensity outside of HAGAs
- Contrast between background intensity and intensity within HAGAs
- Intensity range within HAGAs

References

1. Hoyert DL, Xu JQ. Deaths: preliminary data for 2011. Natl Vital Stat Rep. 2012; 61(6):1–65.
2. Mathers CD, Loncar D. Projections of global mortality and burden of disease from 2002 to 2030. PLoS Med. 2006; 3:e442. [PubMed: 17132052]
3. Scanlon PD, Connett JE, Waller LA, et al. Smoking cessation and lung function in mild-to-moderate chronic obstructive pulmonary disease. Am J Repir Crit Care Med. 2000; 161:381–390.

4. Kanner RE, Connett JE, Williams DE, Buist AS. Effects of randomized assignment to a smoking cessation intervention and changes in smoking habits on respiratory symptoms in smokers with early chronic obstructive pulmonary disease: the Lung Health Study. Am J Med. 1999; 106:410–416. [PubMed: 10225243]

5. Dhariwal J, Tennant RC, Hansell DM, et al. Smoking cessation in COPD causes a transient improvement in spirometry and decreases micronodules on high-resolution CT imaging. Chest. 2014; 145(5):1006–1015. [PubMed: 24522562]

6. Hansell DM, Bankier AA, MacMahon H, et al. Fleischner society: glossary of terms for thoracic imaging. Radiology. 2008; 246:697–722. [PubMed: 18195376]

7. Cosio MG, Hale KA, Niewoehner DE. Morphologic and morphometric effects of prolonged cigarette smoking on the small airways. The American Review of Respiratory Disease. 1980; 122:265–271. [PubMed: 7416603]

8. Gruden JF, Webb WR. CT findings in a proved case of respiratory bronchiolitis. Am J Roentgenology. 1993; 161:44–46.

9. Guckel C, Hansell DM. Imaging the 'dirty lung'—Has high resolution computed tomography cleared the smoke? Clin Radiol. 1998; 53:717–722. [PubMed: 9817087]

10. Heyneman LE, Ward S, Lynch DA, et al. Respiratory bronchiolitis, respiratory bronchiolitis-associated interstitial lung disease, and desquamative interstitial pneumonia: different entities or part of the spectrum of the same disease process? Am J Roentgenol. 1999; 173:1617–1622. [PubMed: 10584810]

11. Moon J, du Bois RM, Colby TV, et al. Clinical significance of respiratory bronchiolitis on open lung biopsy and its relationship to smoking related interstitial lung disease. Thorax. 1999; 54:1009–1014. [PubMed: 10525560]

12. Remy-Jardin M, Edme JL, Boulenguez C, et al. Longitudinal follow-up study of smoker's lung with thin-section CT in correlation with pulmonary function tests. Radiology. 2002; 222:261–270. [PubMed: 11756735]

13. Mastora I, Remy-Jardin M, Sobaszek A, et al. Thin-section CT finding in 250 volunteers: assessment of the relationship of CT findings with smoking history and pulmonary function test results. Radiology. 2001; 218:695–702. [PubMed: 11230642]

14. Hersh CP, Washko GR, Jacobson FL, et al. Interobserver variability in the determination of upper lobe-predominant emphysema. Chest. 2007; 131:424–431. [PubMed: 17296643]

15. Lynch DA, Murphy JR, Crapo JD, et al. A combined pulmonary-radiology workshop for visual evaluation of COPD: study design, chest CT findings and concordance with quantitative evaluation. J Chron Obstruct Pulmon Dis. 2012; 9:151–159.

16. Nakano Y, Muro S, Sakai H, et al. Computed tomographic measurements of airway dimensions and emphysema in smokers. Am J Respirat Crit Care Med. 2000; 162:1102–1108. [PubMed: 10988137]

17. Coxson HO, Dirksen A, Edwards LD, et al. The presence and progression of emphysema in COPD as determined by CT scanning and biomarker expression: a prospective analysis from the ECLIPSE study. The Lancet Resp Med. 2013; 1:129–136.

18. Heussel CP, Herth FJF, Kappes J, et al. Fully automatic quantitative assessment of emphysema in computed tomography: comparison with pulmonary function testing and normal values. Eur Radiol. 2009; 19:2391–2402. [PubMed: 19458953]

19. Regan EA, Hokanson JE, Murphy JR, et al. Genetic epidemiology of COPD (COPDGene) study design. COPD. 2010; 7(1):32–43. [PubMed: 20214461]

20. Xu Y, Sonka M, McLennan G, et al. MDCT-based 3-D texture classification of emphysema and early smoking related lung pathologies. IEEE Trans Med Imaging. 2006; 25:464–475. [PubMed: 16608061]

21. Park YS, Seo JB, Kim N, et al. Texture-based quantification of pulmonary emphysema on high-resolution computed tomography: comparison with density-based quantification and correlation with pulmonary function tests. Invest Radiol. 2008; 43:395–402. [PubMed: 18496044]

22. Sorensen L, Shaker SB, de Bruijne M. Quantitative analysis of pulmonary emphysema using local binary patterns. IEEE Trans Med Imaging. 2010; 29:559–569. [PubMed: 20129855]

23. Ginsburg SB, Lynch DA, Bowler RP, Schroeder JD. Automated texture-based quantification of centrilobular nodularity and centrilobular emphysema in chest CT images. Acad Radiol. 2012; 19:1241–1251. [PubMed: 22958719]
24. Niewoehner DE, Kleinerman J, Rice DB. Pathologic changes in the peripheral airways of young cigarette smokers. N Engl J Med. 1974; 291:755–758. [PubMed: 4414996]
25. McGregor A, Roberts HC, Dong Z. Repeated low-dose computed tomography in current and former smokers for quantification of emphysema. J Comput Assist Tomogr. 2010; 34(6):933–938. [PubMed: 21084912]
26. Ashraf H, Lo P, Shaker SB, et al. Short-term effect of changes in smoking behavior on emphysema quantification by CT. Thorax. 2011; 66:55–60. [PubMed: 20978026]
27. Zach JA, Newell JD Jr, Schroeder J, et al. Quantitative computed tomography of the lungs and airways in healthy nonsmoking adults. Investigative Radiology. 2012; 47(10):596–602. [PubMed: 22836310]
28. Zach JA, Williams A, Jou SS, et al. Current smoking status is associated with lower quantitative CT measures of emphysema and gas trapping. Journal of Thoracic Imaging. 2016; 31(1):29–36. [PubMed: 26429588]
29. Han MK, Kazerooni EA, Lynch DA, et al. Chronic obstructive pulmonary disease exacerbations in the COPDGene study: associated radiologic phenotypes. Radiology. 2011; 261(1):274–282. [PubMed: 21788524]
30. Hastie, T.; Tibshirani, R.; Friedman, J. The elements of statistical learning: data mining, inference, and prediction. New York: Springer; 2001.
31. Becklake MR, Lalloo U. The ‘healthy smoker’: a phenomenon of health selection? Respiration. 1990; 57:137–144. [PubMed: 2274712]
32. Kemerink GJ, Lamers RJS, Pellis BJ, et al. On segmentation of lung parenchyma in quantitative computed tomography of the lung. Med Phys. 1997; 25:2432–2439.
33. Boedeker KL, McNitt-Gray MF, Rogers SR, et al. Emphysema: effect of reconstruction algorithm on CT imaging measures. Radiology. 2004; 232:295–301. [PubMed: 15220511]
34. Genevois PA, Vuyst PD, de Maerelaer V, et al. Comparison of computed density and microscopic morphometry in pulmonary emphysema. Am J Respirat Crit Care Med. 1996; 154:187–192. [PubMed: 8680679]
35. Coxson HO, Rogers RM, Whittall KP, et al. A quantification of the lung surface area in emphysema using computed tomography. Am J Respirat Crit Care Med. 1999; 159:851–856. [PubMed: 10051262]

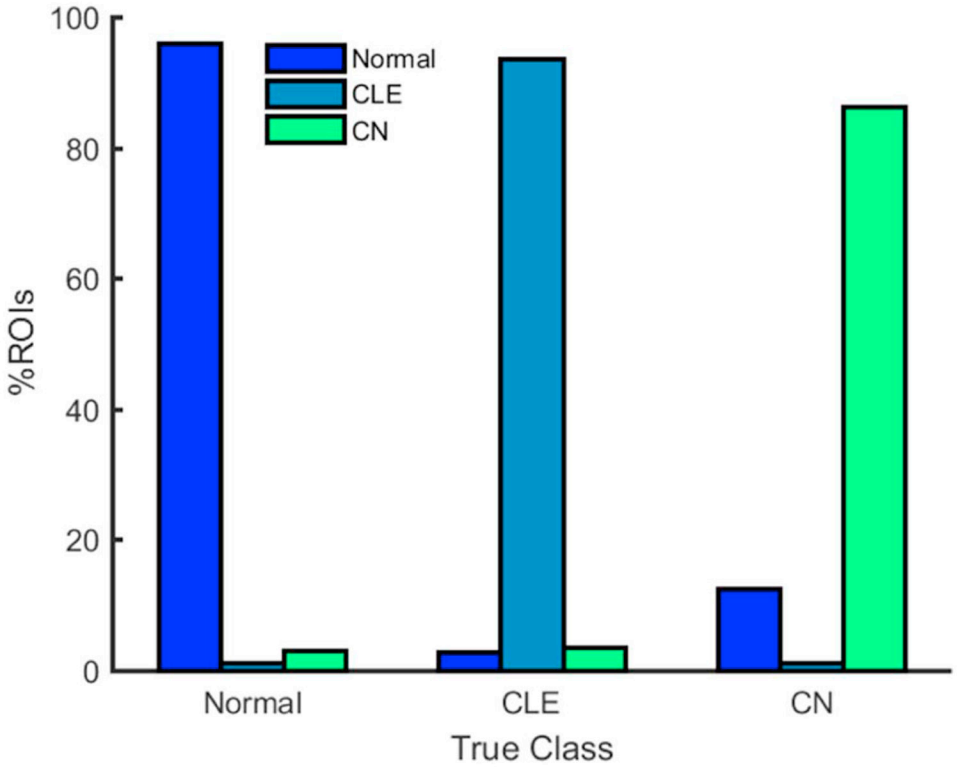

Figure 1. Percentage of ROIs from the training set classified as normal lung, CLE, and CN by the logistic regression classifier

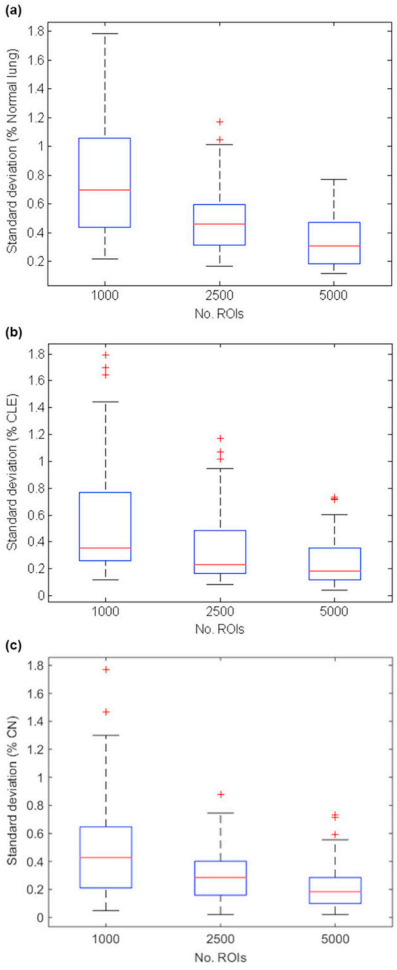

Figure 2.

Standard deviation in (a) % normal lung, (b) % CLE, (c) % CN from 10 repetitions when different numbers of ROIs were randomly selected and classified by the logistic regression classifier. When 5000 ROIs are randomly selected, the standard deviations remain consistently below 1 percentage point.

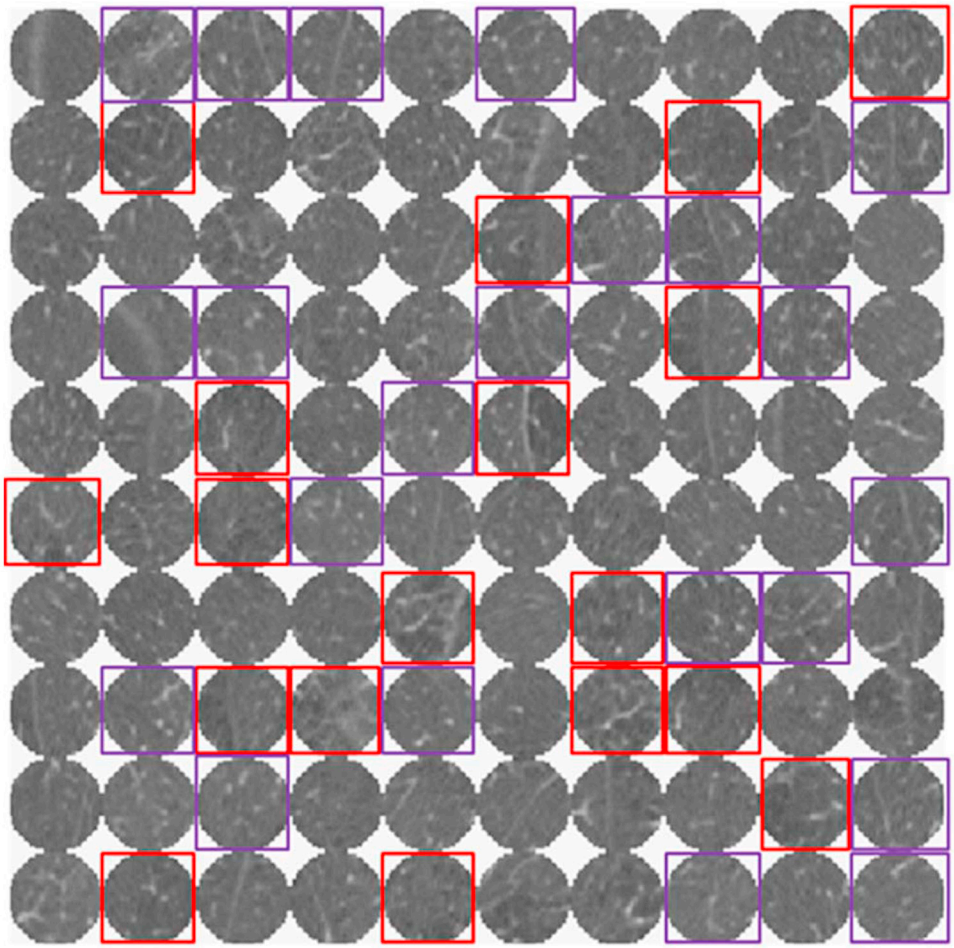

Figure 3. Montage of 100 arbitrarily selected ROIs from a single subject classified as normal lung, CLE (red), or CN (purple) by the logistic regression classifier

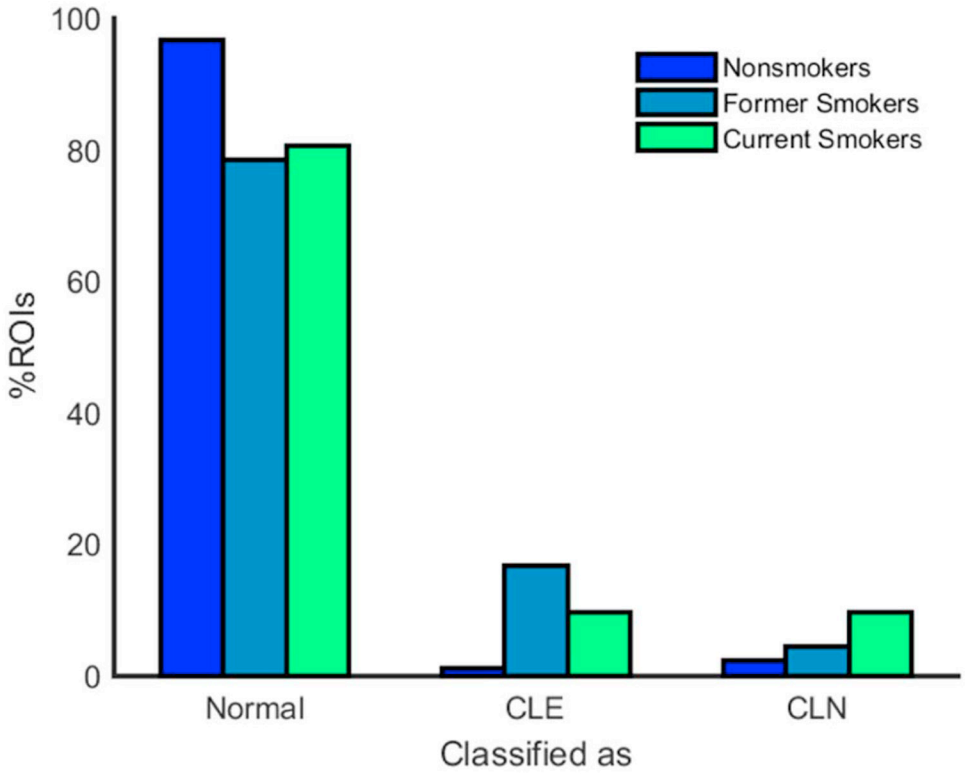

Figure 4.
Percentage and standard deviation of ROIs classified as normal lung, CLE, and CN for nonsmokers, former smokers, and current smokers.

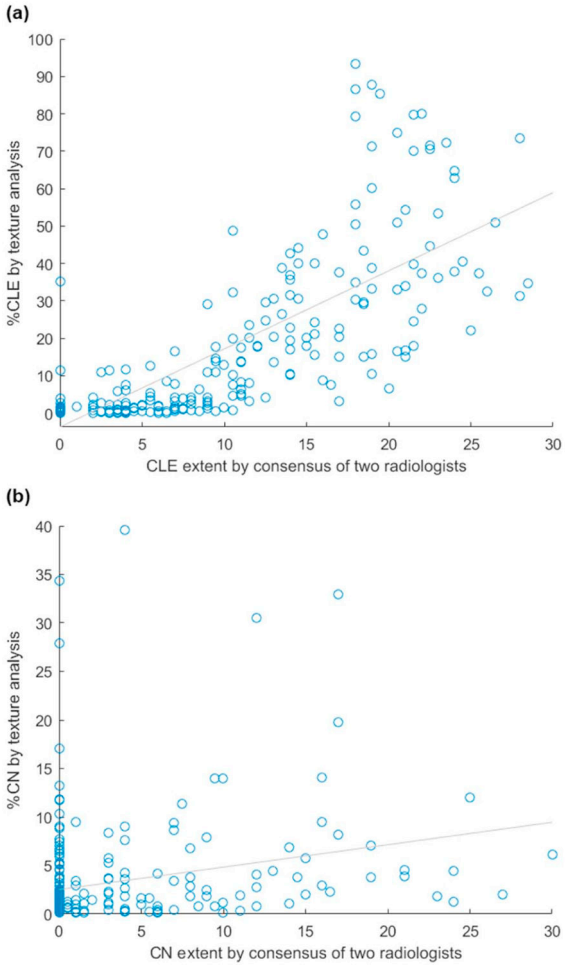

Figure 5.

Scatterplot of (a) CLE extent obtained by a consensus of two radiologists and by texture analysis ($\rho = 0.81$, $p < 0.01$) and (b) CN extent by a consensus of two radiologists and by texture analysis ($\rho = 0.35$, $p < 0.01$).

Table 1

Description of subjects from the COPDGene Study cohort used in this study

	Non-smokers		Former Smokers		Current Smokers	
	Training	**Application**	**Training**	**Application**	**Training**	**Application**
Variable	(n=19)	(n=25)	(n=18)	(n=401)	(n=22)	(n=350)
Subject data						
Men/women	8/11	12/13	9/9	203/198	11/11	173/177
Age at enrollment (y)	63.1±8.0	65.0±9.2	62.1± 8.0	65.3 ± 8.0	56.9 ± 7.3	58.0 ± 8.3
Smoking history						
Cigarettes/day	NA	NA	34.3 ± 14.0	27.4 ±±12.1	17.2 ± 10.1	18.9 ± 10.6
Smoking duration (y)	NA	NA	34.1 ± 13.0	34.5 ± 11.4	41.1 ± 8.2	41.2 ± 8.7
Time since quit (y)	NA	NA	11.6 ± 10.6	13.4 ± 10.9	NA	NA
GOLD stage						
Unclassified	NA	NA	-	64	-	64
0	NA	NA	7	91	4	76
1	NA	NA	2	96	8	90
2	NA	NA	1	92	7	84
3	NA	NA	4	29	3	17
4	NA	NA	4	29	-	19
Scanner						
Siemens Definition	14	11	13	81	11	85
Siemens Definition AS+	1	3	2	27	1	40
Siemens Definition Flash	3	11	1	38	-	28
Siemens Sensation 64	1	-	2	104	10	97
Measurements						
FEV_1	3.0 ± 0.7	2.9 ± 0.8	2.0 ± 1.1	2.3 ± 0.7	2.3 ± 0.8	2.2 ± 0.8
FEV_1% predicted	106.2 ± 11.7	98.9 ± 13.4	66.0 ± 34.1	74.1 ± 23.8	76.9 ± 20.3	76.4 ± 21.7
FEV_1/FVC	0.80 ± 0.05	0.79 ± 0.05	0.55 ± 0.21	0.63 ± 0.15	0.66 ± 0.07	0.66 ± 0.14
% Emphysema *	1.3 ± 0.9	1.7 ± 1.8	14.6 ± 14.8	9.7 ± 10.7	2.4 ± 2.8	5.0 ± 7.7

Acad Radiol. Author manuscript; available in PMC 2017 November 01.

	Non-smokers		Former Smokers		Current Smokers	
	Training	Application	Training	Application	Training	Application
% Gas trapping**	6.6 ± 4.3	7.0 ± 6.0	35.8 ± 24.9	26.2± 19.0	16.9 ± 12.7	18.2 ± 17.5

Data are expressed as mean ± standard deviation or as numbers; NA, not applicable

* Computed as percentage voxels <-950 Hounsfield units on inspiratory CT scans

** Computed as percentage voxels <-856 Hounsfield units on expiratory CT scans

Table 2

Texture-based %CLE and%CN are shown for nonsmokers, former smokers, and current smokers as mean± standard deviation. Two-sample *t*-tests were used to evaluate the statistical significance of differences between groups.

	Non-smokers	Former smokers	Current smokers	*p* (NS vs. FS)	*p* (NS vs. CS)	*p* (FS vs. CS)
% Normal ROIs	96.6±2.7	78.6±23.4	80.6±19.5	$P < 10^{-4}$	$p < 10^{-5}$	$P < 0.21$ *
% CLE ROIs	1.1±1.2	16.9±23.5	9.6±17.0	$P < 10^{-4}$	$P = 0.01$	$p < 10^{-6}$
% CN ROIs	2.3±2.9	4.5±8.4	9.8±13.7	$P < 0.18$ *	$P < 0.01$	$P < 10^{-10}$

NS, nonsmokers; FS, former smokers; CS, current smokers

* Denotes the failure to reject the null hypothesis

Table 3

For 215 subjects with CT scans from both Phases 1 and 2 %CLE and %CN are listed as mean± standard deviation. Two-sample *t*-tests were used to evaluate the statistical significance of differences between Phase 1 and Phase 2 measurements.

	Phase 1	**Phase 2**	***p*-value**
Former smokers in P1 and P2 (n=134)			
% Normal ROIs	79.5±22.8	76.1±27.5	0.27
% CLE ROIs	15.7±22.8	20.9±28.3	0.10
% CN ROIs	4.9±8.5	3.1±5.6	0.04
Current smokers in P1 and P2 (n=52)			
% Normal ROIs	81.5±18.7	77.9±23.3	0.39
% CLE ROIs	8.9±15.9	14.7±22.5	0.13
% CN ROIs	9.7±10.5	7.4±11.5	0.30
Former smokers in P1, current smokers in P2 (n=5)			
% Normal ROIs	78.5±22.4	59.0±42.4	0.39
% CLE ROIs	10.6±16.4	23.0±36.5	0.51
% CN ROIs	10.9±22.1	18.0±37.7	0.72
Current smokers in P1, former smokers in P2 (n=24)			
% Normal ROIs	71.9±25.6	62.5±32.5	0.27
% CLE ROIs	19.4±26.0	29.5±34.4	0.26
% CN ROIs	8.7±16.3	8.0±18.3	0.90

P1, Phase 1; P2, Phase 2

Table 4

Correlations between %CLE and %CN and pertinent variables in 401 former smokers and 350 current smokers. Correlation coefficients and *p*-values were computed using Pearson's correlation.

	Correlation with	
Variable	**%CLE**	**%CN**
Mean of 2 radiologists (n=250)		
CLE extent	0.84 ($p < 0.01$)	NA
CN extent	NA	0.31 ($p < 0.01$)
Densitometry (n=776)		
% Emphysema	0.75 ($p < 0.01$)	-0.29 ($p < 0.01$)
% Gas trapping	0.58 ($p < 0.01$)	-0.34 ($p < 0.01$)
Clinical variables (n=776)		
GOLD stage	0.44 ($p < 0.01$)	-0.30 ($p < 0.01$)
FEV_1	-0.32 ($p < 0.01$)	0.01 ($p = 0.73$)
Time since smoking cessation	-0.16 ($p < 0.01$)	0.07 ($p = 0.16$)
Smoking pack-years	0.26 ($p < 0.01$)	-0.10 ($p = 0.12$)